Molecular and biochemical characterization of *Paragonimus westermani* tyrosinase

Y.-A. BAE[1], S.-H. KIM[1], C.-S. AHN[2], J.-G. KIM[2] *and* Y. KONG[2]*

[1] *Department of Microbiology, Gachon University Graduate School of Medicine, Incheon 406-799, Korea*
[2] *Department of Molecular Parasitology, Sungkyunkwan University School of Medicine, and Center for Molecular Medicine, Samsung Biomedical Research Institute, Suwon 440-746, Korea*

(*Received 22 October 2014; revised 4 December 2014; accepted 8 December 2014; first published online 26 January 2015*)

SUMMARY

Trematode tyrosinases (TYRs) play a major role in the tanning process during eggshell formation. We investigated the molecular and biochemical features of *Paragonimus westermani* TYR (PwTYR). The *PwTYR* cDNA was composed of 1568-bp encompassing a 1422-bp-long open reading frame (474-amino acid polypeptide). A strong phylogenetic relationship with Platyhelminthes and Deuterostomian orthologues was evident. The recombinant PwTYR expressed in prokaryotic cells promptly oxidized diphenol substrates, with a preferential affinity toward *ortho*-positioned hydroxyl groups. It demonstrated fairly weak activity for monophenol compounds. Diphenol oxidase activity was augmented with an increase of pH from 5·0 to 8·0, while monophenol oxidase activity was highest at an acidic pH and gradually decreased as pH increased. Transcription profile of *PwTYR* was temporally upregulated along with worm development. PwTYR was specifically localized in vitellocytes and eggs. The results suggested that conversion of tyrosine to L-dihydroxyphenylalanine by PwTYR monophenol oxidase activity might be rate-limiting step during the sclerotization process of *P. westermani* eggs. The pH-dependent pattern of monophenol and diphenol oxidase activity further proposes that the initial hydroxylation might slowly but steadily progress in acidic secreted vesicles of vitellocytes and the second oxidation process might be rapidly accelerated by neural or weak alkaline pH environments within the ootype.

Key words: *Paragonimus westermani*, tyrosinase, recombinant enzyme, pH-dependent tyrosinase activity, eggshell, vitellocyte.

INTRODUCTION

Paragonimiasis is an inflammatory lung disease caused by the genus *Paragonimus*. A type-species *P. westermani* is prevalent in several Asian countries. Other *Paragonimus* species also invokes human infections in Asia, Africa and America (Lane *et al*. 2009; Fürst *et al*. 2012). Humans are infected by eating raw or undercooked freshwater crustaceans containing infective metacercariae. Consumption of paratenic hosts is also an important route of human infection (Nakamura-Uchiyama *et al*. 2002; Ahn *et al*. 2014). The metacercariae excysted in the duodenum migrate to the lungs through the peritoneal cavity and mature into the oviparous adults approximately 3 months after infection. During the course of chronic infection, eggs trapped in the lungs and other tissues constitute a major component of granuloma and invoke pathophysiological alterations. The eggs may not be resolved even by successful treatment but cause persistent inflammatory and immune responses (Cho *et al*. 2000).

The trematode egg is encapsulated within a cross-linked proteinaceous eggshell, in which a single fertilized ovum is compactly surrounded by numerous vitellocytes (Smyth and Halton, 1983). The vitellocytes matured in vitelline follicles provide resources required for eggshell formation including eggshell precursor proteins and responsible enzyme (s), as well as nutrients for the developing embryo (Threadgold, 1982). Tyrosine residues occupying specific positions are rapidly oxidized into dihydroxyphenylalanine (DOPA) quinone in the ootype (Rice-Ficht *et al*. 1992). The DOPA quinones are subsequently cross-liked to neighbouring tyrosine or lysine residue on adjacent proteins to form a sclerotized eggshell (tanning process) (Cordingley, 1987).

Enzymes classified into the tyrosinase (TYR) (EC 1·14·18·1) regulate multiple biochemical pathways. Their biological implications depend on the taxonomical positions of their donor organisms, with the monophenol (hydroxylation of tyrosine into DOPA) and diphenol oxidase activities (oxidation of DOPA into DOPA quinone) (Jaenicke and Decker, 2004). In mammals, these enzymes play important roles associated with melanin synthesis, wound healing, light adaptation, immune modulation, protein-cross-linking and progression of Parkinson's disease (Olivares and Solano, 2009). In contrast, these proteins are uniquely involved in trematode eggshell formation, by participating in the consecutive oxidation of tyrosine into DOPA quinone in the mature eggshell proteins (Cordingley, 1987). TYR activity was described in *Schistosoma mansoni* (Seed *et al*. 1978), *Schistosoma*

* Corresponding author. Department of Molecular Parasitology, Sungkyunkwan University School of Medicine, Suwon 440-746, Korea. E-mail: kongy@skku.edu

doi:10.1017/S0031182014001942

japonicum (Cai *et al*. 2009), *Fasciola hepatica* (Mansour, 1958) and *Clonorchis sinensis* (Ma, 1963). However, molecular structures and biological significance of the trematode TYRs have only been recently investigated in schistosomes (Fitzpatrick *et al*. 2007; Cai *et al*. 2009; He *et al*. 2012) and *C. sinensis* (Bae *et al*. 2013).

Proteins involved in eggshell formation of *P. westermani* have been reported in only a few studies. Two eggshell precursor proteins, such as Pw-Vit20 and Pw-Vit36 that are highly enriched with glycine, tyrosine, aspartic acid and lysine have been identified. Pw-Vit20 may mediate eggshell maturation while Pw-Vit36 participates in the development of primordial vitelline cells (Bae *et al*. 2007). No other information regarding *P. westermani* eggshell formation is available.

In this study, we determined structural features of a novel cDNA clone putatively encoding *P. westermani* TYR. The egg-shell and vitelline follicle-specific expression of the protein and TYR activity with a preference for diphenol compounds was assessed employing an enzymatically active recombinant protein.

MATERIALS AND METHODS

Parasite samples

Paragonimus westermani metacercariae, collected from naturally infected crayfish in an endemic area of Korea, were orally inoculated into dogs (200 metacercariae/dog). The worms were harvested from the peritoneal cavity (1- and 3-week-old worms) and lungs (7- and 12-week-old worms). The worms were washed more than 10 times with physiological saline at 4 °C. Eggs were collected by incubating adults overnight in phenol red-free RPMI-1640 medium at 37 °C and were purified under a dissecting microscope. Fresh worms and eggs were used in total RNA extraction. Ten fresh adults were fixed in 4% neutral paraformaldehyde. A portion of the worms were stored at −80 °C for protein extraction (Bae *et al*. 2007). Institutional Review Board of Sungkyunkwan University, Korea approved the study protocol (2008-8-18). All animal was housed according to the guidelines provided by the Association for Assessment and Acceleration of Laboratory Animal Care International (Thailand).

Isolation and analysis of a full-length TYR sequence

A partial *TYR*-like cDNA was detected during BLAST analyses of expressed sequence tags (ESTs) of adult *P. westermani* (Bae *et al*. 2007). Oligonucleotide primers were designed to match both ends of the cDNA sequence (5′-CATTGAC AGAGCGCTGGAACTTACC-3′ and 5′-CATCA TGATTGAAGTCCAAAATGGC-3′). In combination with the universal T7 and T3 promoter primers, these primers were applied for PCR-amplification of 3′- and 5′-regions of the gene from an adult cDNA library. After cloning into a pGEM-T Easy vector (Promega, Madison, WI, USA), the nucleotide sequences were automatically determined using a BigDye Terminators Cycle Sequencing Core Kit (Ver. 3·0; Perkin Elmer, Foster City, CA, USA) and an automated ABI PRISM 377A DNA Sequencer (Applied Biosystems, Foster City, CA, USA). A consensus contig was generated by overlapping the 5′- and 3′-region sequences. Its integrity was confirmed by PCR with open reading frame (ORF)-specific primers (5′-ATGGCTATGTCCAAAAAGACACTGG-3′ and 5′-TCAGATGAACACAGGTCCTCCACC-3′).

The putative amino acid sequence of *PwTYR* was predicted by the ORF Finder (http://www.ncbi.nlm.nih.gov/). Similarity pattern was analysed against the non-redundant genomic/proteomic databases of GenBank using the BLAST programs. The putative phosphorylation sites were predicted by NetPhos 2·0 server (http://www.cbs.dtu.dk/services/NetPhos/). The amino acid sequence was also employed as a query during sequence analysis via the Hidden Markov Models (InterProScan, http://www.ebi.ac.uk/Tools/InterProScan/). Presence of hydrophobic signal peptide and transmembrane domain was screened by the SignalP (http://www.cbs.dtu.dk/services/SignalP/) and TMpred (http://www.ch.embnet.org/software/TMPRED_form.html). The PwTYR tertiary structure was simulated by the homology-based ESyPred3D program (http://www.expasy.ch/) and I_TASSER server using the iterative threading assembly refinement algorithm (http://zhanglab.ccmb.med.umich.edu/I-TASSER/). Multiple parameters calculated by the I-TASSER program were used in the statistical validation of the predicted structure (Zhang, 2008).

Generation of recombinant protein and specific antibody

Nucleotide sequence corresponding to the putative mature domain of PwTYR (amino acid positions 122–474) was PCR-amplified from the cDNA library using primers containing *Bam*H I and *Hin*d III restriction sites (5′-CAGGATCCCGAATT CGTAGAGATATTCGA-3′ and 5′-CTAAGCTT TCAGATGAACACAGGTCCTCCACC-3′). The gene segment restricted with the identical enzymes was incorporated into a pET-28a vector (Novagen, Madison, WI, USA). The plasmid was introduced into *Escherichia coli* DH5α cells to verify the expression fidelity by sequencing. The plasmid was inserted into the competent *E. coli* strain BL21 (DE3). The recombinant PwTYR protein (rPwTYR) was induced by incubating the cells in Luria-Bertani medium supplemented with 0·5 mM isopropyl-β-D-thiogalactopyranoside (IPTG) for 4 h at 37 °C. Cells were harvested and sonicated.

https://doi.org/10.1017/S0031182014001942 Published online by Cambridge University Press

The rPwTYR was purified by nickel-nitrilotriacetic acid (Ni-NTA) chromatography (Qiagen, Valencia, CA, USA) under denaturing conditions and monitored by 12% reducing SDS-PAGE (see Fig. A1 in the Appendix).

The rPwTYR protein (30 μg) was mixed with Freund's adjuvants (Sigma-Aldrich, St. Louis, MO, USA) and subcutaneously injected to specific pathogen-free BALB/*c* mice 3 times at 2-week intervals. The mice were boosted with the protein (10 μg) through tail vein. Seven days later, the mice were killed to collect the blood. The blood was centrifuged for 10 min at 3000 ***g***. The rPwTYR-specific mouse antisera were stored at −80 °C until use.

Two-dimensional electrophoresis (2-DE) and Western blotting

Adult *P. westermani* were homogenized in phosphate buffered saline (PBS, pH 7·2) containing a protease inhibitor cocktail (Roche, Mannheim, Germany) using a Teflon-pestle homogenizer. The homogenate was centrifuged at 20000 ***g*** for 30 min and the resulting supernatant was used as adult extracts. Proteins (50 μg) were cleared with trichloroacetic acid and mixed with rehydration buffer containing 6 M urea, 2 M thiourea, 2% CHAPS, 0·4% dithiothreitol (DTT), 0·5% immobilized pH gradient (IPG) buffer and 0·002% bromophenol blue. The mixture was loaded on an IPG strip (pH 3–10; GE Healthcare, Piscataway, NJ, USA) and electrofocused for a total of 35 kVh. The proteins were further resolved by 12% SDS-PAGE gel (160 × 160 × 1 mm) and transferred onto a nitrocellulose membrane (Schleicher & Schuell, Dassel, Germany). The membrane was incubated overnight with the anti-rPwTYR antibody (1:1000 dilution) at 4 °C and subsequently with peroxidase-conjugated anti-mouse IgG antibody (1:2000 dilution; Cappel, West Chester, PA, USA) for 1 h. Signals were detected using enhanced chemiluminescence detection system (ECL; GE Healthcare) after a 2-min exposure.

Assay of enzyme activity

TYR activity in the adult *P. westermani* was observed by in-gel zymography. The adult extracts (50 μg protein) were electrophoresed by 10% native-PAGE at 4 °C. The gels were incubated with 25 mM 4-methylcatechol (4-MC) or tyrosine for 10 min at 37 °C in the presence/absence of a TYR-specific inhibitor, diethyldithiocarbamic acid (DDC; 5 mM). PwTYR activity was detected by 0·3% 3-methyl-2-benzothiazoline hydrochloride (MBTH) dissolved in 90% ethanol.

Purified rPwTYR in 8 M urea (pH 4·5) was incubated at room temperature for 1 h in the presence of 10 mM DTT. The protein was diluted 5 times with an oxidation buffer (50 mM Tris-HCl [pH 8·5], 5 mM cysteine, 1 mM cystine, 5 mM $CaCl_2$, 5 μM $CuSO_4$ and 8 M urea) and left overnight at 4 °C. The denaturing urea was removed by serial dialysis against PBS with step-wise decrease in urea concentration from 6 to 0 M. The protein was further dialysed against phosphate buffer (100 mM, pH 7·0) and centrifuged at 20000 ***g*** for 30 min to remove un-refolded protein aggregate. The refolded rPwTYR was concentrated by lyophilization.

The TYR enzyme activity of native and recombinant proteins was quantitatively determined as described previously (Nellaiappan *et al*. 1989). Adult extracts (100 μg) or rPwTYR (1 μg) was incubated in phosphate buffer (pH 7·0) with various phenol compounds (0·5 mM) and MBTH (0·3%) in a final reaction volume of 200 μl for 5 min at 4 °C. Substrates tested included tyrosine, tyramine and tyrosine methyl ester (TME) for monophenols; hydroquinone (HQ) for *para*-phenol; and L-DOPA, catechol and 4-MC for *ortho*-phenols (Sigma-Aldrich). Absorbance at 488 nm was monitored at 1 min intervals for 7 min using an Infinite M200 spectrophotometer (Tecan, Grödig, Austria). The enzyme activity was expressed as mean ± standard deviation of absorbance change per min per mg protein ($n = 3$). DDC (1 and 10 mM) was supplemented in a series of the reactions. The rPwTYR (0·5 μg) activity against TME and catechol was also measured by changing pH of reaction media from 5·0 to 9·0. The steady-state kinetics of rPwTYR (0·5 μg) was analysed with catechol, L-DOPA and HQ (0·1–10 mM), and were calculated using the SigmaPlot kinetic software (ver. 12·5).

Semi-quantitative reverse transcription-PCR (RT-PCR)

Total RNAs were isolated from different developmental stages of *P. westermani* using TriZol reagents (Invitrogen, Carlsbad, CA, USA). The RNAs were treated with RNase-free DNase (GIBCO BRL, Rockvile, MD, USA). The *PwTYR* transcript in the RNA solutions (1 μg) was amplified into cDNA by RT-PCR employing a primer pair (5′-TCAGATGAACACAGGTCCTCCACC-3′ and 5′-GAATGTGACGAATTCGCCATTTTGG-3′) and a RNA PCR Kit (AMV, ver. 2·1; Takara, Shiga, Japan). The thermal cycling profile included a preheating for 2 min at 94 °C, 25 cycles of 50 s at 94 °C, 1 min at 60 °C, 1·5 min at 72 °C and a final extension for 10 min at 72 °C. The cycling number was empirically determined to insure that the amplification reactions are in their exponential phases. The products were analysed by 1% agarose gel electrophoresis with ethidium bromide staining. *β-actin* gene, whose transcriptional level was shown to be constantly maintained through different developmental stages, was used as a control with a primer pair (5′-GGCCATGTACGTTGCTATCC-3′ and 5′-CAGAGAGAACAGTGTTGGCG-3′).

https://doi.org/10.1017/S0031182014001942 Published online by Cambridge University Press

Immunohistochemical staining

Paragonimus westermani adult worm sections (4 μm-thicknesses) were mounted on electrostatically charged glasses, deparaffinized, rehydrated and rinsed with PBS. The sections were treated for 5 min with 3% hydrogen peroxidase, after which they were blocked for 1 h with 1% BSA. The sections were incubated overnight with the anti-rPwTYR antibody (1:2000 dilution in PBS supplemented with 1% BSA) at 4 °C. Preimmune mouse serum (1:2000 dilution) was employed as a negative control. The slides were further incubated with 1:1000 dilution of goat anti-mouse IgG antibody conjugated with rhodamin (Abcam, Cambridge, UK) and counterstained with 4′,6-diamidino-2-phenylindole (DAPI). The staining patterns were observed using a Meta DuoScan LSM510 confocal fluorescent microscope (Carl Zeiss, Jena, Germany).

RESULTS

Isolation of Paragonimus TYR gene

We had constructed a partial EST database of diverse gene ontologies from a *P. westermani* adult cDNA library (Bae *et al*. 2007). A cDNA clone (#PwEST-98, 681-bp) showed strong sequence similarity with *TYR* genes identified from different organisms (data not shown). A full-length cDNA encompassing the EST clone was isolated from the cDNA library via a series of PCR amplification. The gene, designated *PwTYR*, was composed of 1568-bp and harboured an ORF of 1422-bp (474-amino acid polypeptide). Functional analysis of the theoretically translated amino acid sequence by InterProScan revealed that PwTYR contained conserved typical amino acid sequences for laminin-type epidermal growth factor (EGF)-like (IPR002049) and di-copper centre (IPR008922)/tyrosinase (IPR002227) domains. Critical cysteine and histidine residues involved in disulfide bond formation and copper binding were tightly conserved. In addition, 15 residues putatively modified by phosphorylation (threshold >0·5), such as serine (amino acid positions at 131, 145, 195, 243, 277, 280, 397 and 460), threonine (191 and 383) and tyrosine (152, 193, 262, 417 and 455) were recognized (Fig. 1). Nucleotide sequence data of *PwTYR* was registered in the GenBank under the accession number KM658170.

Structural characteristics of PwTYR

A BLASTx search employing *PwTYR* sequence retrieved several TYR proteins from the non-redundant proteomic databases of GenBank, especially those of Platyhelminthes and Deuterostomia. PwTYR showed 37·3–50·2% sequence identity with schistosome and *Clonorchis* orthologues. Vertebrate TYR-related protein (TYRP) 1 and TYRP2 were also detected (26–28·9% sequence identity). The amino acid conservation was observed throughout entire sequences, rather than being constraint in a distinct block(s). As shown in Fig. 1, functional domains and amino acid residues specific to TYR family were present in PwTYR. The hydrophobic N-terminal segment seemed to act as a signal peptide involved in the cellular localization of the protein. Similar to other trematode orthologues, however, the *Paragonimus* protein did not contain the C-terminal transmembrane domain recognized in vertebrate TYRs and TYRPs (Bae *et al*. 2013). The tertiary structure of PwTYR was predicted by I-TASSER on the basis of homology model (see Appendix, Fig. A2). The program adopted multiple TYR molecules in the protein data bank (PDB) to use as threading templates, such as 2zmy (*Streptomyces castaneoglobisporus*), 3nm8 (*Bacillus megaterium*) and 2p3x (*Vitis vinifera*). A probable model 1 with the highest confidence score (C-score, −2·24) appeared to be statistically significant, considering the template modelling (TM)-score (0·45 ± 0·15) and the root mean square deviation (RMSD) (12·6 ± 4·3 Å). The ESyPred3D program also used the *S. castaneoglobisporus* TYR molecule (1WX2) for the homology modelling. The overall topology and bi-copper active centre (marked with red- and blue-colours in Fig. A2) was relatively well conserved in the tertiary structures of PwTYR and *Streptomyces* TYR (2zmy), with some minor difference including extra loop structures on the surface of the PwTYR molecule (white arrows).

Enzyme characteristics of rPwTYR

We screened the TYR activity of the adult worm extracts employing in-gel zymography. A positive signal was evident in the gel incubated with 4-MC at neutral pH, but this band was completely abolished in the presence of a copper chelator DDC. Tyrosine, a substrate for monophenol oxidase activity did not reveal any detectable reaction (Fig. 2A). A similar finding was also observed by spectrophotometric assay (Fig. 2B). The rPwTYR protein showed substrate specificity similar to that of the native protein; high reactivity against diphenol compounds under neutral conditions (Fig. 2C). The oxidizing activity was greatly influenced by positions of hydroxyl groups. Diphenol compounds with hydroxyl groups at the *ortho*-position of phenol ring, such as L-DOPA, catechol and 4-MC exhibited high reactivity towards rPwTYR; conversely, those with hydroxyl groups at *para*-position (hydroquinone) revealed weak reactivity. The catechol-oxidizing activity, as well as monophenol hydroxylase activity, was dose-dependently inhibited by the presence of DDC (Fig. 2D).

Steady-state kinetic studies demonstrated that the diphenol oxidation reactions intervened by PwTYR

https://doi.org/10.1017/S0031182014001942 Published online by Cambridge University Press

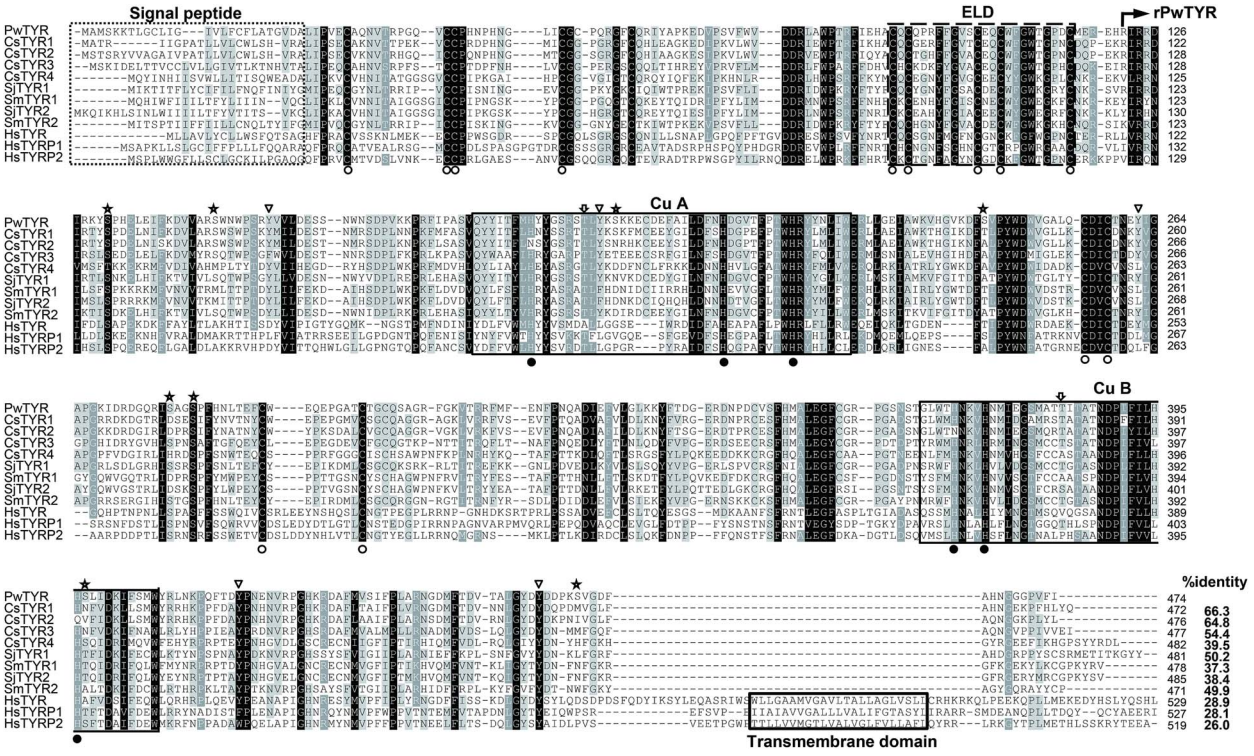

Fig. 1. Structural conservation of PwTYR and its orthologues. The PwTYR primary structure was aligned with those of *C. sinensis* (CsTYR1, KC195913; CsTYR2, KC195914; CsTYR3, KC195915; CsTYR4, KC195916), *S. japonicum* (SjTYR1, AAW26996; SjTYR2, AAW24636) and *S. mansoni* (SmTYR1, AAP93838; SmTYR2, AAW21822) and human tyrosinase (HsTYR, AAB60319) and tyrosinase-related proteins (HsTYRP1, CAG28611; HsTYRP2, AAA20870). Gaps are introduced in the alignment to increase the identity values. Degree of similarity among the proteins for the individual positions is indicated by different shades of gray. Epidermal growth factor-like domain (ELD) is highlighted by a dashed box. Proteolytic cleavage site (start site for expression of recombinant protein) is indicated by an arrow labelled rPwTYR. Tightly conserved di-copper centre (CuA and CuB) and the critical amino acid residues are marked with solid box, open circles (cysteine for disulfide bonds) and solid circles (histidine for copper binding). Putative phosphorylation sites for serine (asterisks), threonine (inverted arrows) and tyrosine (triangles) are also shown. Signal peptide and transmembrane domain are predicted in N- and C-terminal regions, respectively.

followed the Michaelis–Menten equation. Michaelis constants (K_m) for catechol, L-DOPA and hydroquinone at pH 7·0 were calculated to be 0·07, 1·30 and 2·30 mM, respectively (Fig. 3).

Effect of pH on PwTYR activity was monitored by changing pH of reaction solution in a range of 5·0–9·0. Interestingly, the monophenol hydroxylase and diphenol oxidase activities of rPwTYR were reciprocally regulated in accordance with changes of environmental pH (Fig. 4). At an acidic pH, such as 5·0, the monophenol hydroxylase activity was slightly higher than that of diphenol oxidase, although both of enzyme activities were relatively low under given conditions. As pH of the reaction buffer increased, the hydroxylase activity decreased gradually. On the contrary, diphenolase activity was dramatically increased in response to pH increase; the activity reached its plateau at pH 8·0 and declined at pH 9·0.

Spatiotemporal expression pattern of native PwTYR protein

Adult worm extracts (100 µg) were separated by 2-DE, transferred to nitrocellulose membrane and probed with anti-rPwTYR antibody. A strong reactive signal was observed with a protein spot approximately at 53 kDa with a neutral isoelectric point (p*I*), which was shown to have originated from a single protein molecule (Fig. 5A). Molecular weight and p*I* value of the PwTYR matched well with those theoretically calculated from PwTYR sequence (52·2 kDa and 6·19). In addition, we detected a minor spot at ca. 42 kDa (arrow).

When we observed the histological locality of native PwTYR, rPwTYR-specific antibody revealed positive signal exclusively in vitellocytes and eggs (Fig 5B). We assessed the transcription profile of *PwTYR* by semi-quantitative RT-PCR with the total RNAs extracted from various developmental stages of *P. westermani*. *PwTYR* transcription levels were significantly upregulated in accordance with the sexual maturation of worm from 7-week-old to 12-week-old adult (Fig. 5C).

DISCUSSION

In this study, we described molecular and biochemical properties of a novel TYR protein isolated from a lung fluke *P. westermani*. PwTYR contained

https://doi.org/10.1017/S0031182014001942 Published online by Cambridge University Press

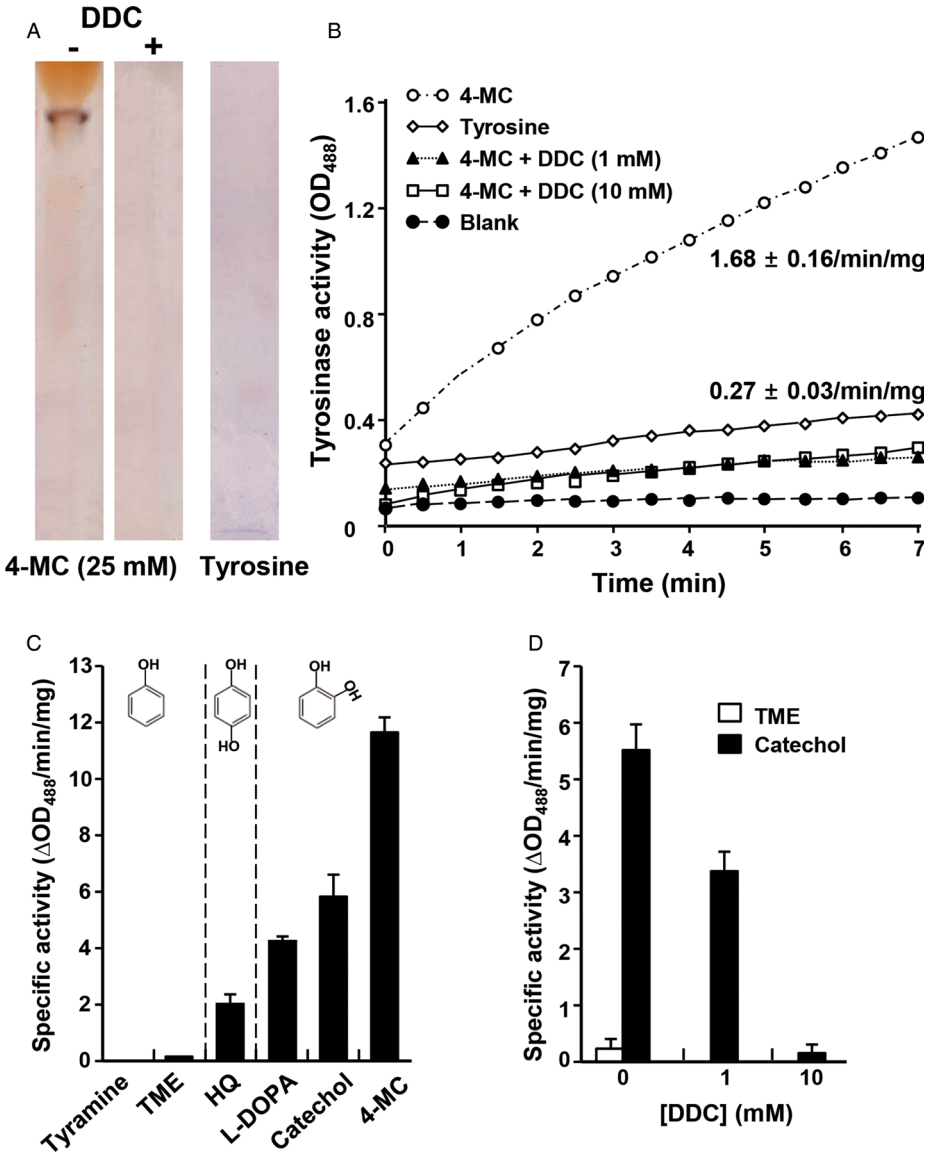

Fig. 2. Biochemical activity of PwTYR. (A) *P. westermani* adult extracts (50 μg each) were resolved by 10% native-PAGE. The gels were incubated with 25 mM 4-MC in the presence (5 mM) or absence of diethyldithiocarbamate (DDC). The reactions were visualized by 0·3% 3-methyl-2-benzothiazoline hydrochloride (MBTH). The gel was also incubated with tyrosine. (B) The PwTYR activity in the adult extracts (100 μg) was incubated in phosphate buffer (pH 7·0) containing 0·3% MBTH with tyrosine or 4-MC in the presence/absence of DDC (1 and 10 mM) for 4 min at 37 °C. Absorbance at 488 nm was monitored at 1 min intervals for 7 min. (C) Enzyme activity of rPwTYR was spectrophotometrically examined under neutral pH condition (7·0) with mono- (tyramine and TME), *para*-phenol (hydroquinone [HQ]) and *ortho*-phenols (L-3,4-dihydroxyphenylalanine [L-DOPA], catechol and 4-methylcatechol [4-MC]). The enzymatic activities, which were expressed as ΔOD_{488} min^{-1} mg^{-1} proteins, are presented as mean ± S.D. of independent triplicate reactions. (D) The specific inhibitory effect of DDC (1 and 10 mM) on the rPwTYR activity was assayed against TME and catechol.

conserved structural motifs including the di-copper centre and amino acid residues involved in the structural stabilization and copper binding. The recombinant protein exhibited strong reactivity against diphenol compounds, but weak activity towards monophenol compounds. Both enzymatic activities were significantly influenced by environmental pH. The vitelline follicle- and egg-specific spatiotemporal distribution of PwTYR correlated well with that of eggshell precursor proteins (Bae *et al*. 2007). *Paragonimus westermani* undergoes rapid sexual maturation between post infection 5- and 7-week in experimental animals and the process is accompanied with the development of vitelline follicles. During this period, expression of eggshell-related protein genes also started to be substantially upregulated (Bae *et al*. 2007). Therefore, PwTYR isolated in this study appears to provide genuine enzyme activity for the eggshell formation.

We observed that only marginal monophenol oxidase activity was detectable in *P. westermani* under neutral pH conditions, compared to the

https://doi.org/10.1017/S0031182014001942 Published online by Cambridge University Press

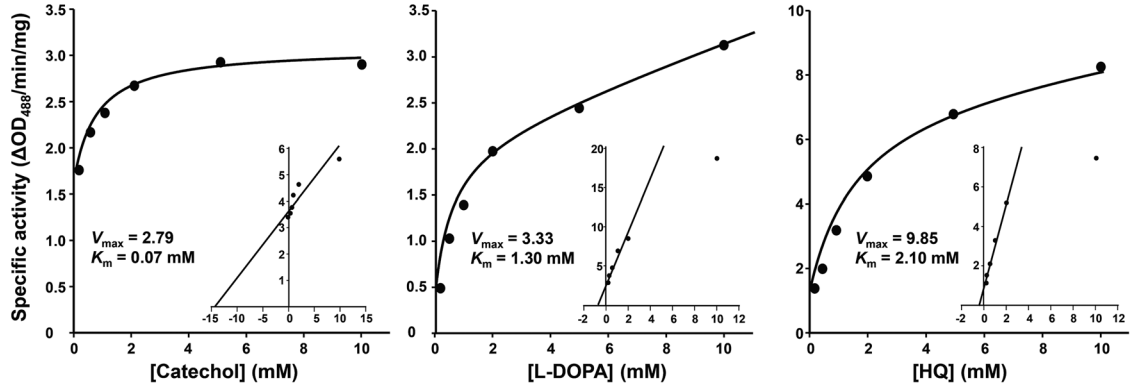

Fig. 3. Michaelis–Menten kinetics of the rPwTYR. The specific activity of rPwTYR was monitored against various concentrations (0·1–10 mM) of catechol, L-3,4-dihydroxyphenylalanine (L-DOPA) and hydroquinone (HQ). The enzyme activity is expressed as ΔOD_{488} min^{-1} mg^{-1} proteins and presented as mean ± S.D. of independent triplicate reactions. Inset panels show Lineweaver–Burk plot of the oxidation reaction. K_m is the Michaelis–Menten constant and V_{max} indicates the maximum reaction velocity.

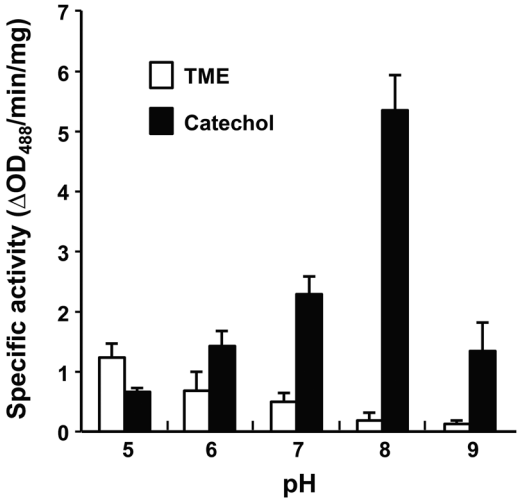

Fig. 4. pH-dependent modulation of monophenol and diphenol oxidase activities of the rPwTYR. The enzymatic activities were spectrophotometrically measured against TME and catechol by changing pH of reaction media (5·0–9·0). The enzymatic activity, which was expressed as ΔOD_{488} min^{-1} mg^{-1} proteins, is presented as mean ± S.D. ($n = 3$).

significant diphenol oxidase activity (Fig. 2). This finding was corroborated with previously described TYR activities of trematode parasites, such as *S. mansoni* (Fitzpatrick *et al*. 2004, 2007), *S. japonicum* (Cai *et al*. 2009) and *C. sinensis* (Bae *et al*. 2013). This observation raised intriguing suggestions either that a second protein other than TYR might be responsible for the essential activity for the generation of DOPA or that the hydroxylase activity of TYR might be affected by a certain kind of physiological factors including ions and pH (Ramalingam, 1970; Wells and Cordingley, 1991). In addition, post-translational modifications including phosphorylation could accelerate the reaction rate of tyrosine hydroxylation (Park *et al*. 1993).

The eggshell proteins and TYRs, which had been co-packaged into vitelline droplets, are secreted from vitellocytes and then accumulated on a template membrane provided by Mehlis' gland in the ootype. After lining the materials along with the membrane, the tanning process might be initiated by the phenol oxidase activity of TYRs (Smyth and Halton, 1983). Therefore, hydroxylation of tyrosine residue might be a rate-limiting reaction, to precisely regulate the biochemical process in a proper time (such as eggshell hardening) or in a specific histological locality (i.e. ootype). The monophenol oxidase activity of PwTYR was much higher in acidic conditions than in neutral/alkaline conditions. It is possible that tyrosine residues of eggshell proteins are slowly but steadily hydroxylated by the lower monophenol oxidase activity in the acidic vesicles of vitellocytes, and thereafter rapidly oxidized into DOPA quinones by the strong diphenol oxidase activity within ootype, in which neutral or weak alkaline pH has maintained. A similar sequential enzymatic process was proposed in *S. mansoni* (Wells and Cordingley, 1991). Alternatively, catechol secreted by Mehlis' gland may act as a cofactor to enhance the monophenol oxidase activity (Smyth and Halton, 1983; Land *et al*. 2003). Previous studies also suggested the presence of a second enzyme(s) for the tyrosine hydroxylation, such as tyrosine hydroxylase (Smyth and Halton, 1983; Marles *et al*. 2003). However, when we considered the finding that similar reaction patterns were observed between native and recombinant proteins (Fig. 2), this possibility might be less likely.

TYR proteins in vertebrates are synthesized as zymogenic forms and converted into active molecules by a selective proteolytic cleavage (Peñafiel *et al*. 1982). Phosphorylation of serine residues by a protein kinase is involved in the activation event (Park *et al*. 1993). Our 2-DE/Western blotting of *P. westermani* proteins with the anti-rPwTYR antibody detected a minor 42-kDa spot with a p*I* value of ca. 5·8, in addition to major 53-kDa protein spot (Fig. 5A). The active form, which was simulated by homology modelling, was predicted to have a molecular weight of 40·8 kDa with p*I* 6·37.

https://doi.org/10.1017/S0031182014001942 Published online by Cambridge University Press

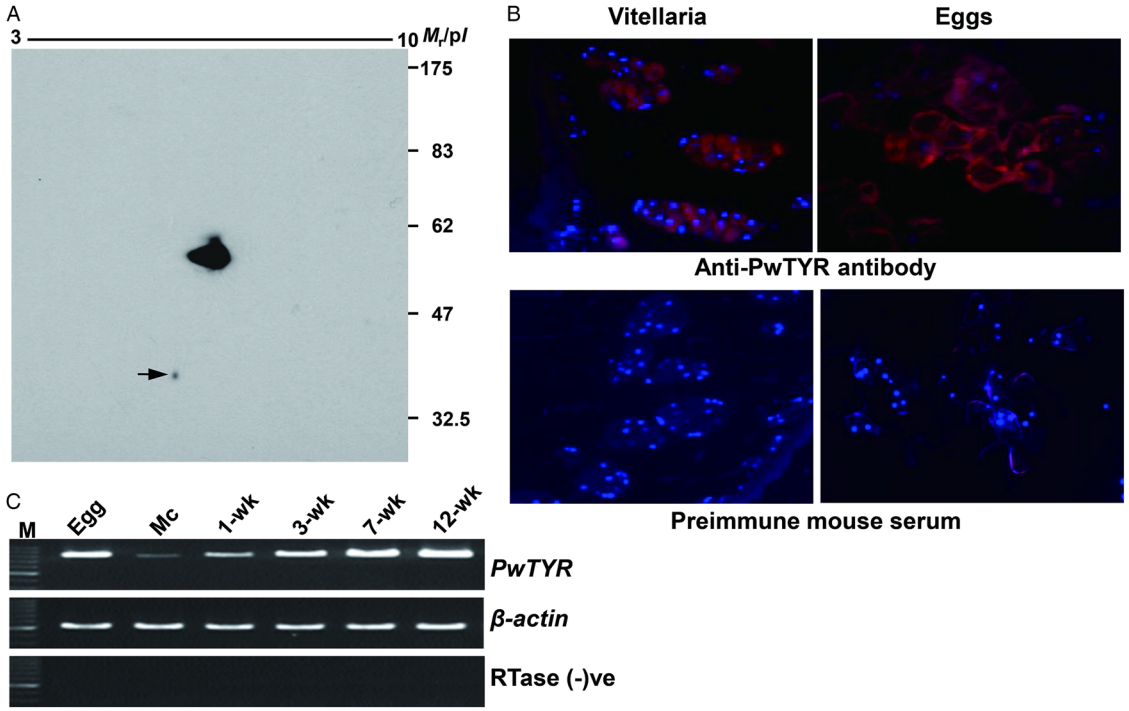

Fig. 5. Expression pattern of PwTYR. (A) *Paragonimus westermani* adult extracts were examined by 2-DE/Western blot analysis with the rPwTYR-specific antibodies. Arrow indicates a protein spot, which might be originated from a fully processed PwTYR. (B) Paraffin-embedded adult worm sections were reacted with the anti-rPwTYR antibody (1:2000 dilution), subsequently with goat anti-mouse IgG antibody conjugated with rhodamin (1:1000 dilution) (upper panel). The worm sections were also probed with preimmune serum and rhodamin conjugated anti-mouse IgG at the same dilution factor (lower panel). The sections were counter stained with DAPI and observed under a fluorescent microscope. (C) mRNA transcripts of the *PwTYR* gene were amplified by reverse transcription-PCR from total RNAs prepared from *P. westermani* in different developmental stages, as indicated on the top in week (wk). Reactions to amplify the β-actin gene were included as an internal standard. RTase (-), reactions depleted reverse transcriptase during the first reverse transcription reaction. M, 100-bp size standards; Mc, metacercaria.

Examination of the mature PwTYR sequence (353 amino acid polypeptide) using the Scansite program (http://scansite.mit.edu/calc_mw_pi.html) demonstrated that 4 (p*I* 5·88) or 5 (5·78) amino acid residues are required to be phosphorylated to get the observed p*I* value. We recognized that 15 sites including 8 serine residues might be putatively phosphorylated through posttranslational modification (Fig. 1). Therefore, the minor spot detected by immunoblotting seems to correspond to the fully processed proteoform of PwTYR including proteolytic cleavage and phosphorylation. Further studies are warranted to elucidate this issue.

In conclusion, the novel TYR protein, which might be involved in the provision of enzyme activity for eggshell formation in *P. westermani*, showed conserved structural features shared by TYR family. The protein demonstrated a strong preferential oxidizing activity to diphenol compounds under neutral and weak alkaline conditions. The mono- and di-phenol oxidase activities are tightly modulated by the pH of surrounding microenvironments. Our data suggested that pH-dependent monophenol and diphenol oxidase activity of PwTYR might be responsible for steady state progression of initial step in acidic vitellocytes and second rapid accelerated oxidation process in alkaline pH conditions within the ootype. We provide a molecular clue to understand regulation of the tanning process in trematode parasites.

FINANCIAL SUPPORT

This work was supported by Ministry of Health and Welfare (Health & Medical Technology R&D Program, Korea, 2008–2009, A084596).

REFERENCES

Ahn, C. S., Na, B. K., Chung, D. I., Kim, J. G., Kim, J. T. and Kong, Y. (2014). Expression characteristics and specific antibody reactivity of diverse cathepsin F members of *Paragonimus westermani*. *Parasitology International* **64**, 37–42.

Bae, Y. A., Cai, G. B., Kim, S. H., Sohn, W. M. and Kong, Y. (2013). Expression pattern and substrate specificity of *Clonorchis sinensis* tyrosinases. *International Journal for Parasitology* **43**, 891–900.

Bae, Y. A., Kim, S. H., Cai, G. B., Lee, E. G., Kim, T. S., Agatsuma, T. and Kong, Y. (2007). Differential expression of *Paragonimus westermani* eggshell proteins during the developmental stages. *International Journal for Parasitology* **37**, 295–305.

Cai, G. B., Bae, Y. A., Zhang, Y., He, Y., Jiang, M. S. and He, L. (2009). Expression and characterization of two tyrosinases from the trematode *Schistosoma japonicum*. *Parasitology Research* **104**, 601–609.

Cho, S. Y., Kong, Y., Yun, D. H., Kang, S. Y., Kim, L. S., Chung, Y. B. and Yang, H. J. (2000). Persisting antibody reaction in paragonimiasis after praziquantel treatment is elicited mainly by egg antigens. *Korean Journal of Parasitology* **38**, 75–84.

Cordingley, J. S. (1987). Trematode eggshells: novel protein biopolymers. *Parasitology Today* **3**, 341–344.

https://doi.org/10.1017/S0031182014001942 Published online by Cambridge University Press

Fitzpatrick, J. M., Hirai, Y., Hirai, H. and Hoffmann, K. F. (2007). Schistosome egg production is dependent upon the activities of two developmentally regulated tyrosinases. *FASEB Journal* **21**, 823–835.
Fitzpatrick, J. M., Johansen, M. V., Johnston, D. A., Dunne, D. W. and Hoffmann, K. F. (2004). Gender-associated gene expression in two related strains of *Schistosoma japonicum*. *Molecular and Biochemical Parasitology* **136**, 191–209.
Fürst, T., Duthaler, U., Sripa, B., Utzinger, J. and Keiser, J. (2012). Trematode infections: liver and lung flukes. *Infectious Disease Clinics of North America* **26**, 399–419.
He, Y., Cai, G., Ni, Y., Li, Y., Zong, H. and He, L. (2012). siRNA-mediated knockdown of two tyrosinase genes from *Schistosoma japonicum* cultured *in vitro*. *Experimental Parasitology* **132**, 394–402.
Jaenicke, E. and Decker, H. (2004). Functional changes in the family of type 3 copper proteins during evolution. *ChemBioChem* **5**, 163–169.
Land, E. J., Ramsden, C. A. and Riley, P. A. (2003). Tyrosinase autoactivation and the chemistry of *ortho*-quinone amines. *Accounts of Chemical Research* **36**, 300–308.
Lane, M. A., Barsanti, M. C., Santos, C. A., Yeung, M., Lubner, S. J. and Weil, G. J. (2009). Human paragonimiasis in North America following ingestion of raw crayfish. *Clinical Infectious Diseases* **15**, e55–e61.
Ma, L. (1963). Trace elements and polyphenol oxidase in *Clonorchis sinensis*. *Journal of Parasitology* **49**, 197–203.
Mansour, T. E. (1958). Effect of serotonin on phenol oxidase from the liver fluke *Fasciola hepatica* and from other sources. *Biochimica et Biophysica Acta* **30**, 492–500.
Marles, L. K., Peters, E. M., Tobin, D. J., Hibberts, N. A. and Schallreuter, K. U. (2003). Tyrosine hydroxylase isoenzyme I is present in human melanosomes: a possible novel function in pigmentation. *Experimental Dermatology* **12**, 61–70.
Nakamura-Uchiyama, F., Mukae, H. and Nawa, Y. (2002). Paragonimiasis: a Japanese perspective. *Clinics in Chest Medicine* **23**, 409–420.
Nellaiappan, K., Devasundari, A. F. and Dhandayuthapani, S. (1989). Properties of phenol oxidase in *Fasciola gigantica*. *Parasitology* **99**, 403–407.
Olivares, C. and Solano, F. (2009). New insights into the active site structure and catalytic mechanism of tyrosinase and its related proteins. *Pigment Cell and Melanoma Research* **22**, 750–760.
Park, H. Y., Russakovsky, V., Ohno, S. and Gilchrest, B. A. (1993). The beta isoform of protein kinase C stimulates human melanogenesis by activating tyrosinase in pigment cells. *Journal of Biological Chemistry* **268**, 11742–11749.
Peñafiel, R., Galindo, J. D., Pedreño, E. and Lozano, J. A. (1982). The process for the activation of frog epidermis pro-tyrosinase. *Biochemical Journal* **205**, 397–404.
Ramalingam, K. (1970). Prophenolase and the role of Mehlis' gland in helminthes. *Experientia* **26**, 828.
Rice-Ficht, A. C., Dusek, K. A., Kochevar, G. J. and Waite, J. H. (1992). Eggshell precursor proteins of *Fasciola hepatica*, I. Structure and expression of vitelline protein B. *Molecular and Biochemical Parasitology* **54**, 129–141.
Seed, J. L., Boff, M. and Bennett, J. L. (1978). Phenol oxidase activity: induction in female schistosomes by *in vitro* incubation. *Journal of Parasitology* **64**, 283–289.
Smyth, J. D. and Halton, D. W. (1983). *The Physiology of Trematodes*. Cambridge University Press, Cambridge, UK.
Threadgold, L. T. (1982). *Fasciola hepatica*: stereological analysis of vitelline cell development. *Experimental Parasitology* **54**, 352–365.
Wells, K. E. and Cordingley, J. S. (1991). *Schistosoma mansoni*: eggshell formation is regulated by pH and calcium. *Experimental Parasitology* **73**, 295–310.
Zhang, Y. (2008). I-TASSER server for protein 3D structure prediction. *BMC Bioinformatics* **9**, 40.

APPENDIX

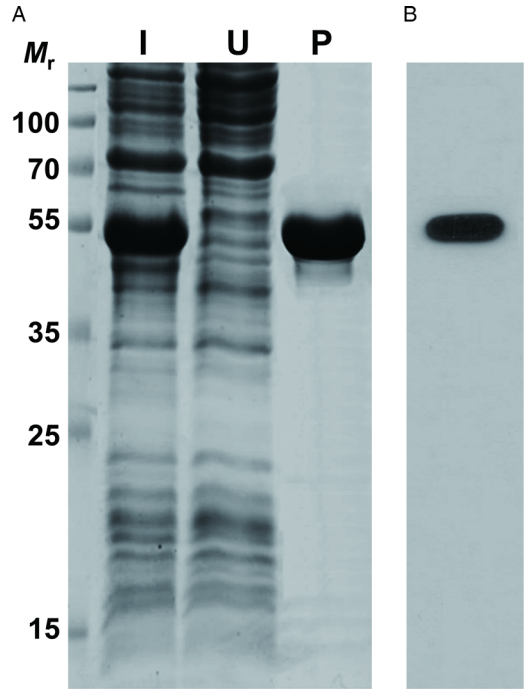

Fig. A1. Expression and purification of the rPwTYR. (A) A *PwTYR* plasmid was inserted into the competent *E. coli* strain BL21 (DE3) and the rPwTYR was induced with IPTG. The rPwTYR was purified by Ni-NTA affinity column. The protein was monitored by 12% SDS-PAGE under reducing conditions. I, cell lysate induced with 0·5 mM IPTG for 4 h at 37 °C; U, uninduced cell lysate; P, purified rPwTYR through Ni-NTA affinity chromatography. M_r, molecular weight in kDa. (B) rPwTYR was probed with murine anti-rPwTYR antibody.

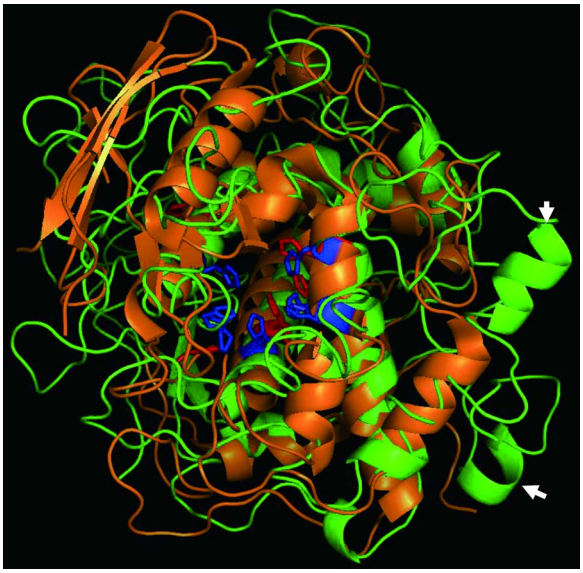

Fig. A2. Comparison of tertiary structures of PwTYR and *S. castaneoglobisporus* TYR. The structures were simulated with homology model-based ESyPred3D program (http://www.expasy.ch/). Green, PwTYR; Orange, 2zmy (*S. castaneoglobisporus*); Red, PwTYR bi-copper centre; Blue, 2zmy bi-copper centre. White arrows indicate extra loop structures found on the surface of the PwTYR molecule.

https://doi.org/10.1017/S0031182014001942 Published online by Cambridge University Press